Design and Solution Structure of Functional Peptide Mimetics of Nerve Growth Factor[||]

Natalia Beglova,[†] Sergei Maliartchouk,[‡] Irena Ekiel,[#] Maria Clara Zaccaro,[‡] H. Uri Saragovi,[‡,§] and Kalle Gehring*[,†]

Department of Biochemistry and Montreal Joint Centre for Structural Biology, Department of Pharmacology and Therapeutics, and Department of Oncology, McGill University, 3655 Promenade Sir William Osler, Montréal, Québec H3G 1Y6, Canada, and Biomolecular NMR Group, Pharmaceutical Biotechnology Sector and Montreal Joint Centre for Structural Biology, Biotechnology Research Institute, National Research Council of Canada, 6100 Royalmount Avenue, Montréal, Québec H4P 2R2, Canada

Received April 4, 2000

The C−D loop in nerve growth factor (NGF) is involved in binding to the NGF receptor, TrkA. It is flexible and adopts several different types conformations in different NGF crystal forms. We have previously shown that a small cyclic peptide derived from the C−D loop of NGF binds to the TrkA receptor by mimicking the structure of this loop. To understand structure−function relationships in NGF C−D loop mimetics, we have produced a series of peptides predicted to form different types of β-turns. The peptides were tested for their ability to promote cell survival in serum-free medium and to induce TrkA tyrosine phosphorylation. NMR structural studies were used to determined the backbone conformation and the spatial orientation of side chains involved in binding to the TrkA receptor. Peptides that form type I or type γL-αR β-turns were the most active. The variety of active loop conformations suggests that the mimetics (and NGF) accommodate the binding site on TrkA by an ′induced fit′ mechanism. In agreement with this hypothesis, NMR relaxation measurements detected both fast and slow motion in the peptides. We also characterized a retro-inverso peptide derived from the NGF C−D loop. This D-amino acid cyclic peptide did not adopt a conformation homologous to the NGF C−D loop and was inactive. This may be representative of difficulties in producing structural and functional mimetics by retro-inverso schemes.

Introduction

Nerve growth factor (NGF) belongs to the neurotrophin family of growth factors.[1,2] It is important for the regulation of neurons during development and in neuron regeneration after injury. Neurotrophins interact with two different transmembrane receptors: Trk and p75.[3−5] TrkA is the NGF-specific tyrosine kinase receptor, whereas the p75 receptor interacts with all members of the neurotrophin family with similar affinity. Both receptors are important for NGF function and cooperate when coexpressed.

NGF and its TrkA receptor are relevant in several pathological states. Target diseases include neuropathies of NGF-dependent neurons,[6−8] therapy of acute nervous system injury such as ischemic stroke and spinal cord injury,[9] and neuroectoderm-derived tumors.[10−12] The high level of proteolytic degradation of proteins and difficulties associated with their administration limit their usefulness as therapeutics. Therefore, it is desirable to search for small peptides and nonpeptidic compounds that bind to selective receptors and either mimic or antagonize neurotrophin activity. Small molecule agonists or antagonists have potential in therapy.[13−16] As a diagonistic tool, TrkA ligands were used to localize TrkA-expressing tumors in vivo[17] and to demonstrate a role for NGF in the maintenance of adult cholinergic neurons.[18]

Turns in protein structure often contain the functionally important residues[19−22] and can serve as templates for developing peptide mimetics. Structure prediction was used to analyze regions in the primary sequence around residues critical for enzyme−substrate specificity. These critical regions appeared to have the propensity for β-turn formation.[23] The β-turns are most common in the binding interfaces of the complexes[24] and are formed by four consecutive residues that determine the preferential type of turn.[25,26] Another advantage of mimicing β-turns in proteins is that turns are generally solvent-exposed and hence turn-derived mimetics are more soluble.

The C−D loop in NGF has been implicated in TrkA receptor binding.[27−29,20] In previous work, we determined the structure of bioactive cyclic NAc-C(92−96) peptide derived from the C−D loop of NGF.[30] The β-turn formed by residues Asp, Glu, Lys, and Gln was induced by disulfide bond formation between cysteines introduced at both termini. This peptide in solution interconverts between two types of β-turns found in different NGF crystal structures.[31−33] The conformational similarity of the peptide and the C−D loop in NGF is most likely the key factor that contributes to the bioactivity of the peptide. Linear peptides derived

* To whom correspondence should be addressed. Tel: (514) 496-2558. Fax: (514) 496-5143. E-mail: kalle.gehring@bri.nrc.ca.
[†] Department of Biochemistry and Montreal Joint Centre for Structural Biology, McGill University.
[‡] Department of Pharmacology and Therapeutics, McGill University.
[§] Department of Oncology, McGill University.
[#] Biotechnology Research Institute.

[||] Abbreviations: NGF, nerve growth factor; NMR, nuclear magnetic resonance; NOE, nuclear Overhauser effect; COSY, correlation spectroscopy; TOCSY, total correlation spectroscopy; SFM, serum-free medium; PY, phosphotyrosine; NAc, *N*-acetyl; MTT, 3-(4,5-dimethylthiazol-2-yl)-2,5-diphenyltetrazolium bromide.

10.1021/jm990441x CCC: $19.00
Published on Web 08/31/2000

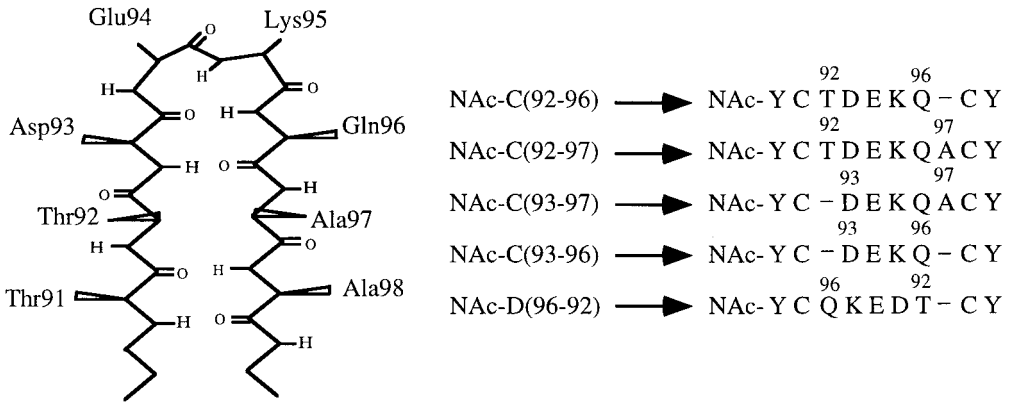

Figure 1. Schematic representation of the C−D loop in NGF and C−D loop-derived peptides.

from the same region are inactive.[27] To further the rational design of small NGF peptidomimetics, we sought to determine which of the two types of C−D loop β-turns detected in solution and crystal structures is active in binding TrkA.

We addressed this problem by designing a new series of peptides. The peptides were designed to form a single type of β-turn around the key residues: Asp, Glu, Lys, and Gln. We expected that an 'alanine scan' of residues in the turn would result in disruption or shift of the turn and eliminate the conformational similarity with the C−D loop, most likely causing the loss of activity. Therefore, we produced peptides that had the primary sequence of the C−D loop but contained a different number of residues between the two cysteines. In this way, the start of the β-turn is maintained at the Asp residue which has high propensity for turn initiation[34] but the type of turn is potentially modified. We also designed a retro-inverso peptide which is obtained by synthesis of a peptide from D-amino acids in reverse order relative to the original peptide. Introduction of D-amino acids in peptide sequences greatly reduces their susceptibility to proteolytic degradation,[35,36] and in some cases retro-inverso peptides maintain the conformation and activity of the parental L-peptides.[37−39] The peptides of varied sizes and the retro-inverso peptide from the C−D loop of NGF were assayed for agonistic mimetic activity induced via TrkA receptors, and their solution structures were determined by NMR. The resulting structure−function relationships in these C−D loop mimetics broadens our understanding of NGF−TrkA binding and can be used in design of future peptidomimetics with improved therapeutic potential.

Results

We studied peptides derived from the C−D loop of NGF. In NGF, this loop connects two antiparallel β-strands via a β-turn formed at the tip of the loop. Peptides were constrained by cyclization through two cysteine side chains and contain an N-terminal acetyl group. The sequence between the cysteines corresponds to the residues 92−97 of mouse NGF. Peptides contained the key residues Asp, Glu, Lys, and Gln that form a β-turn in the C−D loop but differed in the number of residues enclosed between cysteines. The peptides are referred to as NAc-C(92−97), NAc-C(92−96), NAc-C(93−97), NAc-C(93−96), and NAc-D(96−92). NAc-D(96−92) is the retro-inverso analogue of NAc-C(92−96).[30] It contains all D-amino acids linked by normal peptide bonds assembled in inverted order relative to the L-peptide analogue. The peptides all contained N- and C-terminal tyrosine residues that aid during the cyclization reaction and improve bioactivity. A schematic representation of the C−D loop and C−D loop-derived peptides is given in Figure 1.

Structural Information Extracted from the NMR Data. Resonance assignments were made from analysis of 2D ^{1}H homonuclear spectra using conventional methodology.[40,41] We obtained NOE distance restraints from 2D-NOESY spectra with mixing times of 150 and 200 ms. $^3J_{HN-H\alpha}$ and $^3J_{H\alpha-H\beta}$ coupling constants, measured from COSY spectra, were used to constrain the backbone ϕ angles and side-chain χ1 angles. The temperature dependence of the amide proton chemical shift is the characteristic of its protection from solvent exchange. Temperature coefficient values of greater than −3 ppb/K indicate the presence of hydrogen bonds or protection from solvent because of steric shielding; values −3 to −6 ppb/K characterize intermediate protection; and more negative values are typical for fully solvent-exposed amide protons. The temperature coefficients were measured from series of TOCSY spectra over the range of temperatures from 275 to 305 K. In all the peptides, Lys95 and Gln96 have small temperature coefficients indicating solvent protection and a similarly placed β-turn. In the retro-inverso NAc-D(96−92) peptide the smallest temperature coefficients are shifted to residues Glu94 and Asp93 because its sequence is inverted relative to NAc-C(92−96). A summary of the short- and medium-range NOEs, values for $^3J_{HN-H\alpha}$ and $^3J_{H\alpha-H\beta}$ coupling constants, and temperature coefficients for each residue is illustrated in Figure 2A.

Calculated Structures. From 50 structures calculated for each peptide, we chose 20 with the lowest energy and acceptable covalent geometry. Ensembles of structures for each peptide are represented in Figure 2B. Statistics for the NMR structure calculations are summarized in Table 1. Structures are well-defined especially in the loop region between the two cysteine residues where the pairwise rmsd for backbone atoms is less than 0.74 Å and for non-hydrogen atoms is less than 1.2 Å. The average structure calculated for peptides adequately represents the ensemble structures. All the peptides form β-turns comprising residues Asp93, Glu94, Lys95, and Gln96.

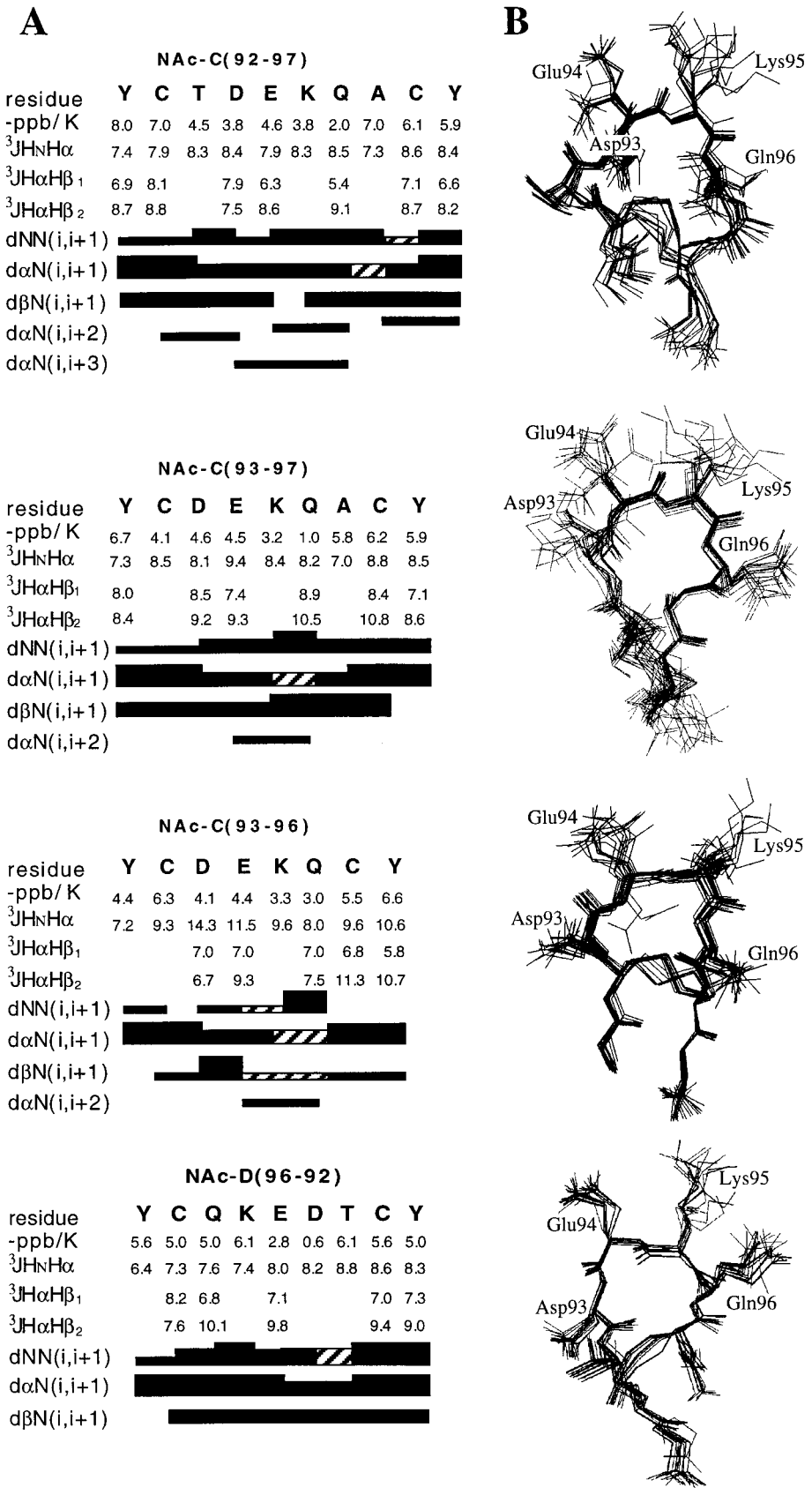

Figure 2. (A) Summary of sequential and medium-range NOE connectivities, scalar coupling values, and amide proton temperature coefficients as observed by NMR spectroscopy for peptides derived from NGF. The top line represents the primary sequence of peptides. The low temperature coefficient values for Lys and Gln residues indicate the presence of a β-turn. Scalar $^3J_{HN-H\alpha}$ and $^3J_{H\alpha-H\beta}$ coupling constants were used to constrain peptide ϕ, $\chi 1$ angles. The horizontal lines represent NOE connectivities with line width indicating the relative magnitude of the observed NOE. Hatched lines indicate NOEs that are missing due to spectral overlap. (B) Ensemble of 20 low-energy structures calculated for each peptide. For clarity, the side chains of the N- and C-terminal tyrosines are not shown.

Table 1. Statistics for the NMR Structure Calculations of the Peptides Derived from NGF

parameter	NAc-C(92−97)	NAc-C(93−97)	NAc-C(93−96)	NAc-D(96−92)
number of residues	10	9	8	9
distance restraints				
number of NOEs (total)	90	61	68	62
sequential	49	34	33	35
i, *i*+2	14	8	6	11
i, *i*+3	5	1	1	1
>*i*, *i*+3	5	4	13	4
number of S−S bond restraints	3	3	3	3
number of dihedral angle restraints (total)	7	5	6	4
ϕ angle restraints	6	5	6	4
χ1 angle restraints	1			
rms deviations (Å) for calculated structures				
all residues:				
backbone atoms	0.84 ± 0.35	0.82 ± 0.27	0.22 ± 0.16	0.50 ± 0.27
non-hydrogen atoms	1.76 ± 0.38	1.89 ± 0.34	1.40 ± 0.44	1.62 ± 0.40
without Tyr termini:				
backbone atoms	0.74 ± 0.31	0.74 ± 0.27	0.22 ± 0.16	0.40 ± 0.23
non-hydrogen atoms	1.04 ± 0.36	1.15 ± 0.37	0.60 ± 0.30	0.67 ± 0.32

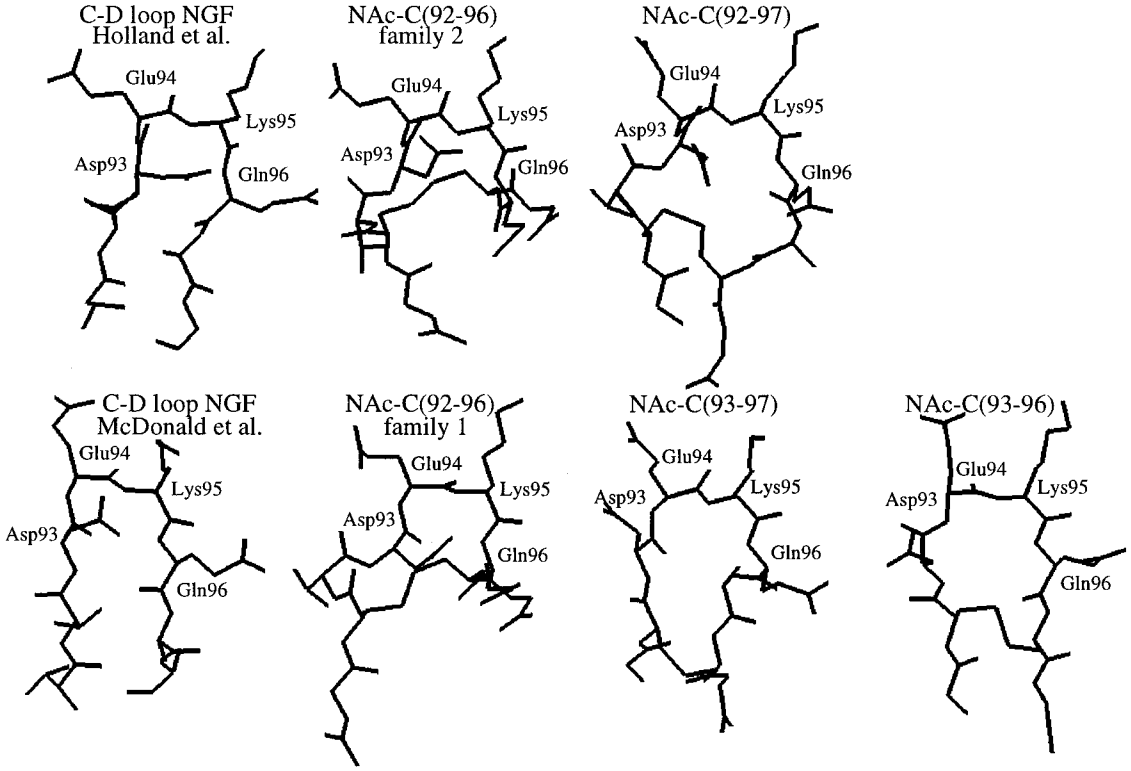

Figure 3. Comparison of energy-minimized average structures calculated for each peptide with the conformation of the C−D loop in NGF from crystallographic data. Backbone and selected side-chain atoms are shown.

In the X-ray structures of NGF, the C−D loop adopts two different types of β-turn: type I and type γL-αR (in the nomenclature of Wilmot and Thornton).[42] As discussed by Beglova et al.[30] the NAc-C(92−96) peptide interconverts between two conformations, each of which corresponds closely to the conformations formed in the native C−D loop. Examination of the new peptide structures reveals that peptide NAc-C(93−97) forms a β-turn similar to the first family of NAc-C(92−96) structures (containing type I β-turns), while peptide NAc-C(92−97) forms a β-turn similar to the second family of NAc-C(92−96) structures (containing γL-αR β-turns). Both of these closely resemble the known conformations of the C−D loop from X-ray crystallography. The NAc-C(93−96) peptide could not be classified into either of these two classes. Figure 3 presents a comparison of the β-turns formed by the C−D loop of NGF with the energy-minimized average peptide structures.

The type of β-turn formed by four consecutive residues is determined by the backbone dihedral ϕ, ψ angles at the second and third residues in the turn. In the L-amino acid peptides NAc-C(92−96), NAc-C(92−97), NAc-C(93−97), and NAc-C(93−96), the β-turn is placed at residues Asp93, Glu94, Lys95, and Gln96. To compare the types of β-turns, we generated Ramachandran plots for Glu94 and Lys95 residues (Figure 4). Each Ramachandran plot represents a superposition of the Glu94 and Lys95 ϕ, ψ angles in the ensemble of 20 structures. The Ramachandran plots readily indicate that a type I β-turn is adopted by the NAc-C(93−97) and NAc-C(92−96) family 1 peptides. The NAc-C(92−97) and NAc-C(92−96) family 2 peptides form a γL-αR β-turn. NAc-

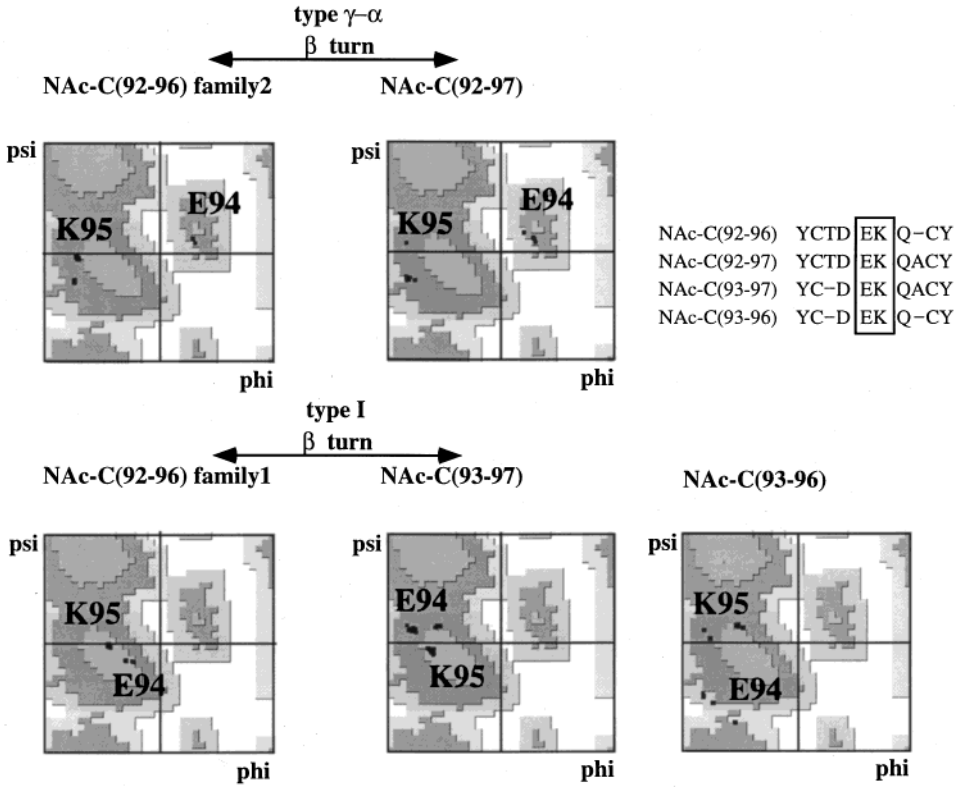

Figure 4. Ramachandran plots presenting the distribution of ϕ, ψ dihedral angles for residues Glu94 and Lys95 in peptides derived from the C−D loop in NGF. The ϕ, ψ backbone angles of these residues [positions (i+1), (i+2)] determine the type of β-turn formed.

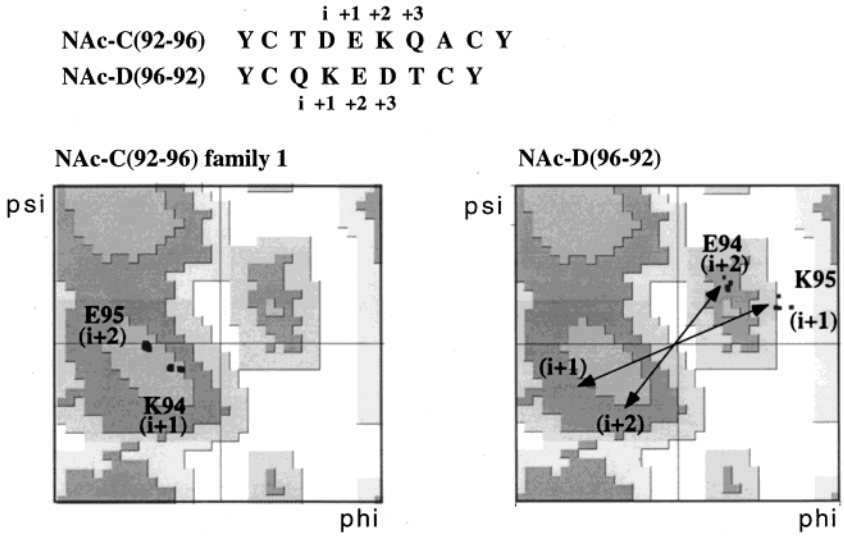

Figure 5. Ramachandran plots presenting the ϕ, ψ backbone angles of (i+1) and (i+2) residues in the all L-amino acid peptide NAc-C(92−96) and the retro-inverso NAc-D(96−92) peptide. The arrows illustrate the mirror image transformation associated with accessible regions for D- versus L-amino acids.

C(93−96) could be referred to as a degenerate or conformationally strained type I β-turn. Both type I and γL-αR β-turns are found in X-ray crystal structures of the C−D loop of NGF.[31−33]

We calculated the structure of the retro-inverso NAc-D(96−92) peptide. It forms a β-turn that comprises residues Gln96, Lys95, Glu94, and Asp93 (numbered according to the NGF sequence). The small temperature dependence of the Asp93 amide proton indicates shielding from solvent and confirms the position of the β-turn at Lys95−Glu94. Figure 5 shows Ramachandran plots for the L-amino acid NAc-C(92−96) peptide and the D-amino acid NAc-D(96−92) peptide. As might be expected, the backbone angles for the retro-inverso peptide are opposite in sign compared to the L-amino acid peptide.[43] This mirror image interconvertion generates a type I′ β-turn[44] (also termed a $\gamma\gamma$-turn[42]). The ϕ, ψ angles of residues (i+1), (i+2) of NAc-D(96−92) are located in an allowed region for D-amino acids corresponding to a left-handed α-helix.

Relaxation Properties of the Peptides. To compare the flexibility of the peptides, we analyzed the motion of the Cα−Hα bond vector by measuring NMR relaxation times and the ^{13}C−^{1}H heteronuclear NOEs

Table 2. Experimentally Measured R_1, R_2 Relaxation Rates, NOE Enhancements, and Calculated NMR Relaxation Parameters for Methine Carbons of Bioactive Peptides Derived from NGF[a]

residue	R_1 (1/s)	R_2 (1/s)	NOE	S^2	τ_ϵ (ps)	R_{2exch} (1/s)
			NAc-C(92−97): $\tau_m$opt= 1.94 ns			
Tyr	4.0 ± 0.2	6.8 ± 0.3		0.40 ± 0.07	320 ± 108	
Cys	3.9 ± 0.2	14.0 ± 0.6		0.88 ± 0.05		4.4 ± 0.8
Thr92	3.6 ± 0.1	12.7 ± 0.5		0.78 ± 0.03		4.0 ± 0.6
Asp93	4.0 ± 0.2	15.2 ± 0.9		0.90 ± 0.05		5.3 ± 1.1
Glu94	3.9 ± 0.1	14.6 ± 0.5		0.87 ± 0.04		5.0 ± 0.7
Lys95	3.6 ± 0.1	10.5 ± 0.5		0.80 ± 0.03		1.7 ± 0.6
Gln96	3.9 ± 0.2	13.3 ± 0.4		0.87 ± 0.06		3.7 ± 0.7
Ala97	3.7 ± 0.1	8.8 ± 0.5		0.80 ± 0.03		
Cys	3.8 ± 0.2	9.7 ± 0.5		0.86 ± 0.03		
Tyr	3.5 ± 0.2	8.3 ± 0.3		0.75 ± 0.02		
Thr93β	3.2 ± 0.2	10.1 ± 0.4		0.69 ± 0.06		2.3 ± 0.8
			NAc-C(93−97): $\tau_m$opt = 1.78 ns			
Tyr	4.0 ± 0.2	7.0 ± 0.2		0.48 ± 0.06	285 ± 79	
Cys	4.1 ± 0.2	9.1 ± 0.3		0.88 ± 0.03		
Asp93	4.1 ± 0.2	15.2 ± 0.4		0.89 ± 0.05		5.9 ± 0.6
Glu94	4.1 ± 0.2	13.0 ± 0.5		0.88 ± 0.05		3.8 ± 0.67
Lys95	3.9 ± 0.2	25.7 ± 1.7		0.85 ± 0.06		16.8 ± 1.8
Gln96	4.6 ± 0.2	17.5 ± 1.1		0.98 ± 0.02		7.1 ± 1.2
Ala97	4.0 ± 0.1	9.1 ± 0.4		0.86 ± 0.02		
Cys	4.1 ± 0.2	9.1 ± 0.3		0.88 ± 0.03		
Tyr	3.9 ± 0.1	6.5 ± 0.2		0.42 ± 0.04	256 ± 39	
			NAc-C(93−96): $\tau_m$opt = 1.62 ns			
Tyr	4.1 ± 0.1	11.9 ± 0.3	0.40 ± 0.03	0.78 ± 0.02	98 ± 21	3.9 ± 0.4
Cys	3.9 ± 0.2	9.3 ± 0.3	0.28 ± 0.04	0.82 ± 0.05		1.2 ± 0.5
Asp93	4.6 ± 0.2	20.3 ± 0.6	0.29 ± 0.03	0.95 ± 0.04		10.9 ± 0.7
Glu94	4.1 ± 0.1	19.2 ± 0.8	0.31 ± 0.04	0.84 ± 0.03		10.8 ± 0.9
Lys95	4.2 ± 0.1	11.8 ± 0.2	0.45 ± 0.04	0.77 ± 0.03	163 ± 53	3.6 ± 0.4
Gln96	4.3 ± 0.1	9.3 ± 0.2	0.35 ± 0.02	0.84 ± 0.02	103 ± 28	0.8 ± 0.3
Cys	4.1 ± 0.1	11.6 ± 0.3	0.31 ± 0.05	0.85 ± 0.03		3.1 ± 0.4
Tyr	4.0 ± 0.1	8.0 ± 0.1	0.46 ± 0.05	0.76 ± 0.02	127 ± 35	

[a] The overall rotational correlation time was optimized for each peptide during the last round of calculations.

of backbone α-carbons in the peptides. From the experimental data, we calculated Lipari and Szabo parameters which describe the dynamics of the bond vector on different time scales. Table 2 presents experimentally measured R_1, R_2 relaxation rates for the methine carbons. Preliminary calculations for model selection were carried with the overall isotropic correlation time τ_m fixed at the value obtained for the NAc-C(92−96) peptide.[30] In the last round of calculations the overall rotational correlation time was optimized simultaneously for all residues. The optimized value of the overall rotational correlation time is 1.94 ns for NAc-C(92−97), 1.78 ns for NAc-C(93−97), and 1.62 ns for NAc-C(93−96). This is in good agreement with the value of 1.81 ns previously obtained for the NAc-C(92−96) peptide and reflects the dependence of the rotational correlation time on molecular size.

For the NAc-C(92−97) and NAc-C(93−97) peptides, it was possible to describe the experimentally obtained R_1 and R_2 relaxation rates with motion on two time scales. The motion of the NAc-C(93−96) peptide is more complex and for some residues could not be described by only two types of motion. To better describe the motional dynamics, we measured the carbon−proton heteronuclear NOEs for this peptide (Table 2).

As expected, the terminal tyrosines of all the peptides are very flexible and characterized by picosecond time scale motion and low S^2 order parameters. The C-terminal tyrosine of NAc-C(92−97) does not show this type of motion because it is restricted by the participation of its amide proton in a hydrogen bond with the backbone oxygen of Ala97. In this peptide, a second hydrogen bond is formed between the carbonyl oxygen of the N-terminal Cys and the amide proton of Glu94 with a NH−O distance of 2.7 ± 0.2 Å, a N−O distance of 3.6 ± 0.2 Å, and a N−H−O angle of 159° ± 4°.

Our data suggests that all the peptides form well-defined structures as indicated by the high values of the order parameter S^2 but that they also undergo slow millisecond time scale motion. This motion is cooperative and involves several neighboring residues. This conformational exchange most likely occurs between similar conformations because the measured NMR NOE and dihedral angle constraints could be simultaneously satisfied in a single structural model.

Specific Peptides Afford Partial Agonism in Trophic Assays. One of the biological functions of NGF is to rescue cells from apoptotic death induced by culture in serum-free media (SFM). Untreated SFM cultures resulted in apoptosis unless cells were supplemented with NGF. NGF at 1 nM concentrations affords optimal protection and was used as a positive control (100% survival).[45−47]

Previously, it was demonstrated that the peptide NAc-C(92−96) affords partial survival of cells expressing TrkA and p75 receptors in SFM.[47] Partial agonism was seen when the peptide was applied in synergy with MC192, a monoclonal antibody ligand of p75 receptors. MC192 alone had no significant activity. We set out to compare the activity of the different peptide analogues of NAc-C(92−96) using the same paradigm.

The cell lines 6-24 (Figure 6) and 4-3.6 (data not shown) which express high levels of TrkA and p75 ($TrkA^{2+}$ $p75^{2+}$) were used. The peptides NAc-C(92−97), NAc-C(92−96), NAc-C(93−97), and NAc-C(93−96) afforded partial protection from apoptosis in synergy with MC192. Protection ranged from 20% to 45% compared to 1 nM NGF. In contrast, untreated and linear peptide-

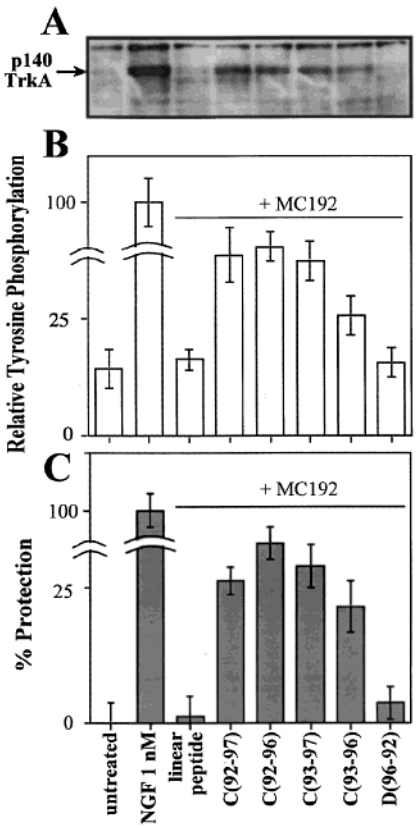

Figure 6. (A) Equal amounts of protein from whole cell lysates were resolved by SDS−PAGE and analyzed by Western blotting with anti-PY mAb 4G10. Blot shown is representative of six independent experiments. 6-24 cells were untreated (lane 1) or treated with indicated ligands (10 μM) for 15 min at 37 °C. (B) Densitometric scanning quantification of TrkA PY intensities relative to optimal NGF treatment (average ± SEM, $n = 6$). (C) Cell viability was quantitated using the MTT colorimetric assay. Percent protection from apoptosis was standardized from MTT optical density (OD) readings at 595 nm relative to optimal (1 nM) NGF = 100%. The OD values of control untreated samples were subtracted and were always <20% of 1 nM NGF.

treated cells underwent apoptosis, and the retro-inverso NAc-D(96−92) peptide afforded very little or insignificant protection (Figure 6C). Data are shown for 10 μM peptide which is the concentration that afforded maximal survival.

Tests with PC12 cells that express lower TrkA levels ($TrkA^+$ $p75^{2+}$) gave similar results; overall survival was lower but statistically significant (data not shown). In B104 cells that do not express TrkA ($TrkA^-$ $p75^{2+}$), no protection was detected (data not shown) confirming that the bioactivity of the peptides requires TrkA expression.

To confirm that the peptides afford partial cell survival by the induction of TrkA phosphorylation, receptor tyrosine phosphorylation (PY) was studied in 6-24 cells in response to a 15-min treatment with the test peptides. A representative anti-PY Western blot is shown in Figure 6A. A summary of densitometric analysis from several blots is given in Figure 6B. Data were compared with tyrosine phosphorylation induced by 1 nM NGF. Treatment with linear peptide controls or with the NAc-D(96−92) retro-inverso peptide did not result in an increase of TrkA tyrosine phosphorylation compared to untreated cells. Treatment with NAc-C(92−97), NAc-C(92−96), and NAc-C(93−97) afforded nearly 40% relative tyrosine phosphorylation, and treatment with NAc-C(93−96) afforded 25% of maximal response. These phosphorylation data following short-term treatment with ligands are consistent with survival data which was obtained after treatment with ligands for 3 days.

Discussion

NGF has a wide range of potential therapeutic applications. To be useful as a pharmacological agent, it would be advantageous to reduce NGF to a small mimetic that is resistant to proteolysis, is orally bioavailable, and is absorbed into tissues of interest. Both NGF antagonists and agonists could be useful. Thus, we studied peptides derived from the C−D loop of NGF which is known to interact with the TrkA receptor.[27,48−50]

In NGF, the C−D loop is flexible and adopts different types of β-turn as revealed by X-ray crystal structures.[31−33] To study the structure−function relationships, we made peptides that formed different types of turns and compared their bioactivity. We chose a design that maintained the key residues that form the β-turn but changed the number of residues enclosed between the two cyclizing cysteines. The use of a side-chain disulfide bond for cyclizing the peptide constrains the cysteine side chains to be located on the same side of the incipient β-sheet. We reasoned that altering the size of the cyclic peptide would alter the position of the cysteine side chains and influence the type of β-turn formed.

To measure activity, we assayed peptides for their ability to activate TrkA and to protect cells from apoptotic death. As shown previously, our results indicate that peptide and antibody mimics of NGF can exhibit partial agonistic activity in the absence of NGF.[45−47] They act through the activation of the TrkA receptor and provide trophic support. The active peptides do not directly dimerize the receptor but, most likely, cause conformational changes on TrkA that stabilize receptor dimerization. In a similar fashion, a small molecule mimic of granulocyte-colony-stimulating factor was recently reported to activate the G-CSF receptor both in vitro and in vivo.[51]

Similar TrkA activity was found for all the peptides containing at least five amino acids between the cysteines [i.e. NAc-C(92−96), NAc-C(93−97), and NAc-C(92−97)]. The peptides form either type I or γL-αR type turns, and both types of β-turn appear to be sufficient for binding and activating TrkA. Even though ϕ, ψ angles in these two types of turns are quite different (Figure 4), the overall conformation of the turn is similar. In both the mimetic peptides and NGF, the C−D loop is quite flexible and likely accommodates the TrkA binding pocket upon binding. Further adaptation to the receptor is accomplished by the long Lys and Gln side chains. In the three peptides, the position of the β-turn is maintained at residues Asp93, Glu94, Lys95, and Gln96. This conserved structure reflects the high propensity of Asp and Glu to initiate β-turns; alternatively positioned turns have significantly lower turn potentials.[34] Comparison of the peptide sequences shows that the threonine and alanine residues preceding and following the β-turn are clearly dispensable for TrkA binding, while the four turn residues appear to be essential.

The smallest peptide, NAc-C(93−96), displayed somewhat less activity than the longer peptides both in the TrkA phosphorylation assay and in the MTT anti-apoptotic assay (Figure 6). Structural analysis of NAc-C(93−96) revealed a strained type I β-turn conformation with ϕ, ψ angles for residue Glu94 at the edge of typical values. This suggests that this peptide cannot adjust to the TrkA binding site to the same degree as the longer peptides, resulting in weaker binding and/or efficacy. Analysis of NMR relaxation in NAc-C(93−96) also indicated more complex motion than in the longer peptides (Table 2). The limited number of observable data relative to model parameters makes further speculation about the significance of this motion difficult. It should be noted that the peptides were all modeled assuming isotropic tumbling and the addition of anisotropic rotation might alter the size of the τ_ϵ and $R_{2\text{exch}}$ motional parameters.

Small peptides are usually susceptible to proteolytic degradation. While cyclization and chemical modifications, such as N-terminal acetylation, substantially increase their resistance to proteolysis,[52] the introduction of D-amino acid anomers provides a further increase in the peptide half-life.[35,36] For this reason, we prepared the retro-inverso analogue of NAc-C(92−96). Like the L-amino acid peptides, the retro-inverso NAc-D(96−92) peptide forms a β-turn comprising residues Gln, Lys, Glu, and Asp. However, this peptide is without significant activity in either of the biological assays.

Comparison of the structures of the retro-inverso NAc-D(96−92) peptide and active L-amino acid peptides shows that the conformations are very different. The NAc-D(96−92) forms a type I′ β-turn which is a mirror image of the type I family of NAc-C(92−96) and NAc-C(93−97) structures (Figure 5). As β-turn propensities are not direction-independent, it is not obvious that the turn would form where it does, and in fact, shifting of the β-turn to include threonine markedly increases the calculated β-turn potential.[34] Type I′ β-turns are typical for D-amino acids, and the upper right quadrant in the Ramachandran plot for D-amino acids corresponds to a favorable α-helical backbone conformation. A recently reported NMR structure of the retro-inverso analogue of a right-handed α-helix showed that the retro-inversion converted it into a left-handed helix.[53]

In the retro-inverso peptide, the β-turn occurs at the first residue following the first cysteine. This is not true for NAc-C(92−96) but is the case for the NAc-C(93−97) peptide. Comparison of the overall shape of NAc-C(93−97) and NAc-D(96−92) shows a striking mirror image symmetry (Figure 7). Alignment of the structures to superimpose the glutamate and lysine reveals a complete inversion in the orientation of the aspartate and glutamine residues. To approach this issue more quantitatively, we calculated the torsion angle defined by the four Cα atoms of the β-turn ($C\alpha^{Asp}-C\alpha^{Glu}-C\alpha^{Lys}-C\alpha^{Gln}$). This torsion angle reflects a screw axis for the β-turns. Since type I and I′ β-turns correspond to half-turns of α-helices, these correspond to right- and left-handed helices. For NAc-C(93−97), the torsion angle is positive (approximately 75°) and corresponds to a right-handed helix. All of the L-amino acid peptides, with the exception of NAc-C(93−96), showed right-handed turns with large torsion angles (51° and 84°). On the other hand, for the retro-inverso peptide, this angle is negative (approximately −60°) and describes a left-handed helix. Inversion of the peptide sequence changes the positions of the amino acid side chains but does not alter the handedness of the β-turn formed so that the angle is the same whether measured from Asp to Gln or from residue i to (i+3). The handedness of the turn depends primarily on the chirality of the amino acid residues and not on the amino acid sequence.

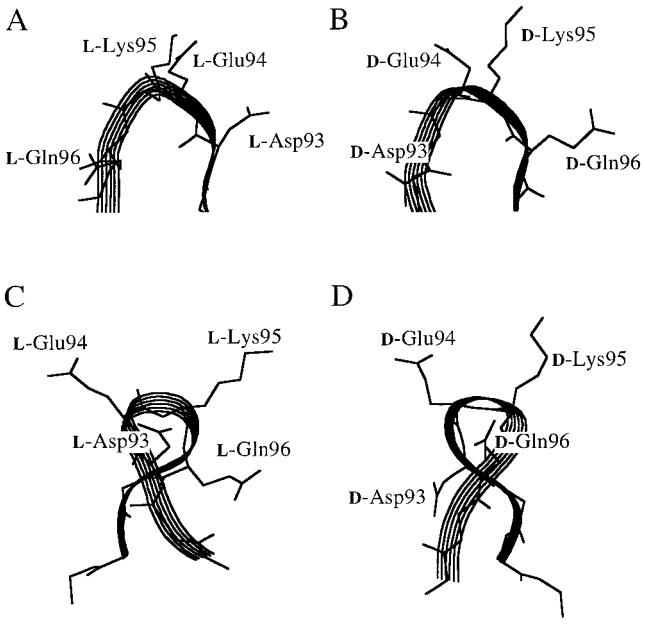

Figure 7. Comparison of orthogonal projections of the energy-minimized average structure of the all-L-amino acid peptide NAc-C(93−97) (panels A, C) and the retro-inverso NAc-D-(96−92) peptide (panels B, D). Side-chain atoms are shown only for the β-turn residues. The structures can be seen to have opposite handedness so that the backbone fold of the retro-inverso peptide is the mirror image of NAc-C(93−97). In particular, the spatial orientation of the Glu, Lys, and Gln side chains is very different which explains the lack of activity for the retro-inverso peptide.

This important change in backbone geometry is accompanied by alterations in the orientation of the side-chain atoms. In the peptide structures, the backbone conformation and Cβ orientations are well-determined and these orientations can be used to quantitate the structural differences observed between the active and inactive peptides. We measured the relative orientation of the side chains of residues from the torsion angle θ formed by two Cα−Cβ bonds projected along the line through the Cα atoms. While for many side-chain pairs this angle was similar in all the peptide structures, a major difference was detected for the glutamate and lysine amino acids at the tip of the β-turn (Figure 8). In the active mimetics, this angle varies between 44° and 81°. For the partially active NAc-C(93−96) mimetic, the angle is −9°, and for the inactive retro-inverso, the angle is −72°. This difference between the L-amino acid and D-amino acid peptides reflects the different types of β-turns. In type I β-turns, the Cβ atom of residue (i+1) assumes an equatorial position, while the (i+2) Cβ is in an axial position (up). In type I′ β-turns, the (i+1) Cβ is again equatorial but the (i+2) is in an axial position (down).[44] Thus, the torsion angles formed by the Cα-Cβ vectors are different and result in very different relative side-chain orientations.

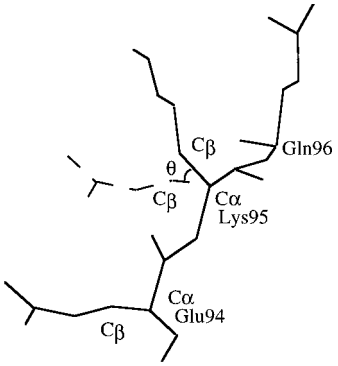

peptide	angle θ (degree)
NAc-C(92-96)	
family 1	59 +/- 2
family 2	52 +/- 4
NAc-C(92-97)	44 +/- 10
NAc-C(93-97)	81 +/- 7
NAc-C(93-96)	-9 +/- 32
NAc-D(96-92)	-72 +/- 5

Figure 8. Relative orientation of Glu94 and Lys95 side chains was assessed from the torsion angle θ formed by the Cα−Cβ bonds of Glu94 and Lys95 ($C\beta^{Glu}-C\alpha^{Glu}-C\alpha^{Lys}-C\beta^{Lys}$). The insert presents the range of θ values measured for each ensemble of 20 peptide structures. Essentially identical results were obtained for the Cα−Cα−Cα−Cα torsion angle described in the text. On the other hand, the torsion angle between the Cα−Cβ bonds of Lys95 and Gln96 was very similar (14−64°) in all the peptide structures (active and inactive).

These large structural differences between the retro-inverso peptide and the most active L-amino acid mimetics suggest that it is the relative orientation of several residues which are important for binding to and activating TrkA. Mutagenesis and analysis of the biological properties of an NT-3/NGF chimeric molecule have identified NGF residues Lys95 and Gln96 and possibly Glu94 as important for receptor binding and activation.[54,28,55] In order for TrkA to discriminate between left-handed and right-handed β-turns, at least four points must contact TrkA. Given the flexible nature of the long side chains, it appears likely that the TrkA recognizes at least three residues, most likely Glu94, Lys95, and Gln96. Additionally, it is quite possible that backbone atoms participate in hydrogen bonds with the receptor and that the exchange of position between amide and carbonyl atoms in the retro-inverso peptide leads to further loss of activity.

The recent X-ray crystal structure of NGF with a fragment (domain 5) of the TrkA receptor gives an idea about where the C−D loop binds.[31] In the crystal structure, the C−D loop is free and does not make contacts with domain 5 of TrkA. Instead, the loop points toward the putative membrane face where it could bind to the 40-amino acid linker sequence that connects domain 5 with the TrkA transmembrane domain. This model is supported by genetic evidence that mutations in this linker in TrkA decreased NGF binding while similar mutations in TrkC had no effect on binding of NT-3.[56] In the absence of the transmembrane helix, this linker may not be folded as it is proteolytically sensitive.[31] Using NMR (Beglova et al., unpublished results), we have been unable to detect binding of the peptide mimetics to the soluble TrkA extracellular domain.[57,58]

Conclusions

Our design has allowed us to prepare peptides that form either of two active conformations present in the native C−D loop in NGF. Structure−activity correlation of the designed peptides revealed that the turn conformation at the Asp, Glu, Lys, and Gln residues is important to ensure an appropriate orientation of the side chains that contact the receptor. The bioactive cyclic peptides closely resemble the conformation of the C−D loop in NGF. Our results suggest that some flexibility in the C−D loop in NGF is allowed and that the loop binds to the receptor by an 'induced fit' mechanism. The designed peptides could serve as a scaffold for the new generation of mimetics with improved properties. A similar design approach could be used to produce small peptide mimetics of other neurotrophin β-turns.

Our structural analysis of an inactive retro-inverso mimetic of the C−D loop of NGF reveals that the absence of activity results from the improper spatial orientation of multiple recognition elements. Despite its sequence inversion, the all D-amino acid peptide formed a structure that was the mirror image of the active L-amino acid mimetics. This suggests that even the smallest secondary structural elements of proteins (β-turns) may not be amenable to retro-inversion. It remains a possibility that mimicking type II or β-turns that form more planar structures by retro-inverso peptides might be more successful.

Experimental Procedures

Peptide Synthesis, Oxidation, and Mass Spectroscopy. *N*-Acetylated peptides were synthesized by the solid-phase method on a model 396 Multiple Peptide Synthesizer (Advanced ChemTech) using a standard Fmoc procedure. They were purified on a preparative Vaydac C18 column using Waters high-pressure liquid chromatography. Peptides were designed to mimic residues T92, D93, E94, K95, Q96 and A97 in the primary sequence of the C−D loop of NGF. Synthetic peptides were referred to as NAc-C(92−97), NAc-C(93−96) and NAc-C(93−97). Purified peptides were oxidized under dilute conditions, repurified and lyophilized. Cysteine residues of linear control peptides were blocked by incubation with 6-fold excess of iodoacetamide at room temperature for 30 min and repurified.

Mass spectrometry was used to assess peptide composition after synthesis and possible dimerization upon oxidation as described previously.[30] No dimers were detected. The measured masses of oxidized and reduced peptides exactly corresponded to expected values.

NMR Spectroscopy and Structure Calculations. For homonuclear experiments, the sample contained 5−15 mM peptide in 10% or 100% (v/v) D_2O/H_2O, pH 5.6, 275 K. Spectra were acquired at 500 MHz proton frequency on a three-channel Bruker DRX500 spectrometer equipped with pulse field gradients. Spectra were acquired and processed as discussed.[30]

The NOE cross-peak intensities, $^3J_{HN-H\alpha}$ and $^3J_{H\alpha-H\beta}$, coupling constants were converted into distance and dihedral angle restraints.[30] Structures were calculated with the hybrid distance geometry−dynamical simulated annealing protocol[59−61] implemented in X-PLOR.[62]

An ensemble of 50 structures was calculated for each peptide. Final acceptance of the structures were based on the following covalent geometry criteria: no bond length violations greater than 0.05 Å, a bond length violation rmsd of less than 0.01 Å, no valence angle violations greater than 5°, an angle violation rmsd of less than 2°, and no improper violations greater than 5°. Criteria for the existence of a hydrogen bond were a donor−acceptor distance of less than 3.6 Å and a donor−proton−acceptor angle of more than 120°.[63]

NMR Relaxation Measurements and Calculation of Relaxation Parameters. All heteronuclear NMR experiments were done at natural ^{13}C abundance with an 10−18 mM sample in D_2O, pH 5.6, 275 K containing 10 mM EDTA. The ^{13}C chemical shifts were determined from a $^{13}C/^1H$ HSQC.[64] The relaxation measurements were done on backbone methine carbons as described by Palmer and colleagues.[65] R_1 measurements were obtained from 10 experiments with relaxation delays (T) of 0.006, 0.05, 0.10, 0.15, 0.40, 0.50, 0.70, 0.9, 1.3

and 1.8 s. For R_2 relaxation measurements, the spin−echo delay between 180° pulses was 5 ms. Ten experiments were performed with relaxation delays (T) of 5, 15, 30, 50, 75, 100, 126, 176, 226 and 276 ms. To estimate the steady-state ^{1}H−^{13}C NOE, two spectra were recorded: one with broad-band ^{1}H saturation to obtain the NOE enhancement, the other without ^{1}H saturation. The recovery delay in the heteronuclear NOE experiments was 4 s. Errors for calculated heteronuclear NOE values were estimated from signal-to-noise ratios obtained from saturated and unsaturated spectra. The ^{1}H−^{13}C NOE enhancements and R_1, R_2 relaxation rates were calculated from the experimental data as described previously.[30]

The R_1, R_2 dipolar relaxation rates and NOE enhancements were used to characterize dynamics of the backbone in solution. Lipari and Szabo formalism allows the extraction of three parameters: S^2, τ_ϵ, and $R_{2\text{exch}}$, each representing a particular time scale of the methine carbon motion.[66] The value of the order parameter S^2 describes the fastest motion on less than a picosecond time scale and reflects the amplitude of backbone tumbling around its equilibrium position. The value of S^2 varies from 1 for completely restrained internal motion to 0 for isotropic unrestrained internal motion. The internal correlation time τ_ϵ describes motion on a picosecond−nanosecond time scale. Values of τ_ϵ above 100 ps indicate increased motion on a picosecond time scale and usually correlate with large heteronuclear NOEs, small values of R_1, and decreased order parameters, S^2. The $R_{2\text{exch}}$ parameter describes the slow motion on a microsecond−millisecond time scale. The conformational exchange contributes to that type of motion.

Dynamic parameters were calculated from the experimentally measured relaxation data with the Modelfree 3.1 program.[65] The R_1, R_2 and NOE experimental data for each residue were fit using different combinations of relaxation parameters: S^2 alone, S^2 and τ_ϵ, S^2 and $R_{2\text{exch}}$, or all three parameters S^2, τ_ϵ, and $R_{2\text{exch}}$.[67] In the last run of calculations, the global rotational correlation time τ_m was optimized.

Cell Lines. PC12 rat pheochromocytomas cells express low levels of rat TrkA and 40 000−100 000 p75 receptors/cell ($TrkA^+$ $p75^{2+}$). B104 rat neuroblastoma cells express ∼50 000 p75 receptors/cell but do not express Trks ($TrkA^-$ $p75^{2+}$). The 4-3.6 cells are B104 cells stably transfected with human *trkA* cDNA and express equal surface levels of p75 and TrkA ($TrkA^{2+}$ $p75^{2+}$).[68] The 6-24 cells are PC12 cells stably transfected with human *trkA* cDNA and overexpressing TrkA ($TrkA^{2+}$ $p75^{2+}$).[69] Cell surface expression of each of NGF receptors was routinely controlled in all cells by quantitative FACScan assays (Becton Dickinson, CA).

Antibody Preparation. Anti-rat p75 IgG mAb MC192 was purified from ascites.[70] MC192 binds to p75 with nanomolar affinity irrespective of expression and binding of TrkA NGF receptors.

Protection from Apoptosis. 5000 cells/well in protein-free media (PFHM-II, GIBCO, Toronto) containing 0.2% bovine serum albumin (BSA) (crystalline fraction V, Sigma, St. Louis, MO) were seeded into 96-well plates (Falcon, Mississauga, Ontario). The cultures were untreated or treated with serial dilutions of NGF (Prince Labs, Toronto). Test agents included IgG MC192 and cyclic peptides; negative controls included mouse IgG (Sigma) or linear peptides. Peptides were tested at 10 μM. Cell viability was quantitated using the MTT colorimetric assay (3-(4,5-dimethylthiazol-2-yl)-2,5-diphenyltetrazolium bromide) after 56−72 h of culture. Percent protection from apoptosis was standardized from MTT optical density (OD) readings at 595 nm relative to optimal (1 nM) NGF = 100%. The OD values of control untreated samples were subtracted and were always <20% of 1 nM NGF. Apoptotic death in SFM (as opposed to necrotic death) was confirmed by analysis of DNA fragmentation patterns (data not shown).

Tyrosine Phosphorylation Assays. Prior to activation, cells were rested for 30 min in SFM to lower baseline TrkA phosphorylation. Cells were then treated with the indicated agent(s) for 15 min and lysed. The tyrosine phosphorylation state of TrkA was assessed by Western blots of whole cell lysates, developed with the enhanced chemoluminescence system (Amersham, Oakville, Ontario). Anti-phosphotyrosine (α-PY) mAb 4G10 (UBI, New York) was used as a primary antibody. Quantitation of protein loading was done with the Bio-Rad detergent compatible protein assay (Bio-Rad Laboratories) and by Coomassie blue staining of gels. Bands in photographic films were quantified by densitometry and intensities were standardized relative to 1 nM NGF. Statistical analysis of densitometry of six blots was done by paired Student's *t*-tests.

Acknowledgment. We thank Hervé Hogues for help in calculating NMR relaxation rates. This work was supported by the National Cancer Institute of Canada Grant 10334 to K.G. and a Canadian Medical Research Council grant to H.U.S. NRC publication 42957.

References

(1) Chao, M. V. Neurotrophic receptors: a window into neuronal differentiation. *Neuron* **1992**, *9*, 583−593.
(2) Davies, A. M. The role of neurotrophins in the developing nervous system. *J. Neurobiol.* **1994**, *25*, 1334−1348.
(3) Chao, M.; Casaccia-Bonnefil, P.; Carter, B.; Chittka, A.; Kong, H.; Yoon, S. O. Neurotrophin receptors: mediators of life and death. *Brain Res. Rev.* **1998**, *26*, 295−301.
(4) Carter, B.; Lewin, G. R. Neurotrophins live or let die: does p75NTR decide? *Neuron* **1997**, *18*, 187−190.
(5) Kaplan, D. R.; Miller, F. D. Signal transduction by the neurotrophin receptors. *Curr. Opp. Cell. Biol.* **1997**, *9*, 213−221.
(6) Lee, S. E.; Shen, H.; Taglialatela, G.; Chung, J. M.; Chung, K. Expression of nerve growth factor in dorsal root ganglion after peripheral nerve injury. *Brain Res.* **1998**, *796*, 99−106.
(7) Hefti, F. Neurotrophic factor therapy for nervous system degenerative diseases. *J. Neurobiol.* **1994**, *25*, 1418−1435.
(8) Connor, B.; Dragunow, M. The role of neuronal growth factors in neurodegenerative disorders of the human brain. *Brain Res. Rev.* **1998**, *27*, 1−30.
(9) Shigeno, T.; Mima, T.; Takakura, K.; Graham, D. I.; Kato, G.; Hashimoto, Y.; Fukukawa, S. Amelioration of delayed neuronal death in the hippocampus by nerve growth factor. *J. Neurosci.* **1991**, *11*, 2914−2919.
(10) Muragaki, Y.; Chou, T. T.; Kaplan, D. R.; Trojanowski, J. Q.; Lee, V. M.-Y. Nerve growth factor induces apoptosis in human medulloblastoma cell lines that express trkA receptors. *J. Neurosci.* **1997**, *17*, 530−542.
(11) Kramer, K.; LeSauteur, L.; Saragovi, H. U.; Cheung, N. K. Characterization of TrkA protein expression in human neuroblastomas. *Adv. Cancer Res.* **1996**, *2*, 1361−1367.
(12) Marchetti, D.; McQuillan, D.; Spohn, W.; Carson, D.; Nicolson, G. Neurotrophin stimulation of human melanoma cell invasion: selected enhancement of heparanase activity and heparanase degradation of specific heparan sulfate subpopulations. *Cancer Res.* **1996**, *56*, 2856−2863.
(13) McInnes, C.; Sykes, B. D. Growth factor receptors: structure, mechanism, and drug discovery. *Biopolymers* **1997**, *43*, 339−366.
(14) Maliartchouk, S.; Feng, Y.; Ivanisevic, L.; Debeir, T.; Cuello, A. C.; Burgess, K.; Saragovi, H. U. A designed peptidomimetic agonistic ligand of TrkA nerve growth factor receptors. *Mol. Pharmacol.* **2000**, *57*, 385−391.
(15) Saragovi, H. U.; Gehring, K. Development of pharmacological agents for targeting neurotrophins and their receptors. *Trends Pharmacol. Sci.* **2000**, *21*, 93−98.
(16) Hefti, F. Pharmacology of neurotrophic factors. *Annu. Rev. Pharmacol. Toxicol.* **1997**, *37*, 239−267.
(17) LeSauteur, L.; Cheung, N.-K.; Lisbona, R.; Saragovi, H. U. Small molecule imaging of nerve growth factor receptors in vivo. *Nat. Biotechnol.* **1996**, *14*, 1120.
(18) Debeir, T.; Saragovi, H. U.; Cuello, A. C. A nerve growth factor mimetic TrkA antagonist causes withdrawal of cortical cholinergic boutons in the adult rat. *Proc. Natl. Acad. Sci. U.S.A.* **1999**, *96*, 4067−4072.
(19) Daopin, S.; Piez, K. A.; Ogawa, Y.; Davies, D. R. Crystal structure of Transforming Growth Factor-β2: an unusual fold for the superfamily. *Science* **1992**, *257*, 369−373.
(20) Ibanez, C. F. Emerging themes in structural biology of neurotrophic factors. *Trends Neurosci.* **1998**, *21*, 438−444.
(21) Oefner, C.; D'Arcy, A.; Winkler, F. K.; Eggiman, B.; Hosang, M. Crystal structure of human platelet-derived growth factor BB. *EMBO J.* **1992**, *11*, 3921−3926.
(22) Schlunegger, M. P.; Grutter, M. G. An unusual feature revealed by the crystal structure at 2.2 A resolution of human transforming growth factor-β2. *Nature* **1992**, *358*, 430−434.

(23) Murakami, M. Critical amino acids responsible for converting specificities of proteins and for enhancing enzyme evolution are located around β-turn potentials: data-based prediction. *J. Protein Chem.* **1993**, *12*, 783−789.
(24) Wilson, I. A.; Stanfield, R. L. Antibody−antigen interactions: new structures and new conformational changes. *Curr. Opin. Struct. Biol.* **1994**, *4*, 857−867.
(25) Dyson, H. J.; Rance, M.; Houghten, R. A.; Lerner, R. A.; Wright, P. E. Folding of immunogenic peptide fragments of proteins in water solution. I. Sequence requirements for the formation of a reverse turn. *J. Mol. Biol.* **1988**, *201*, 161−200.
(26) Wilmot, C. M.; Thornton, J. M. Analysis and prediction of the different types of β-turn in proteins. *J. Mol. Biol.* **1988**, *203*, 221−232.
(27) LeSauteur, L.; Wei, L.; Gibbs, B. F.; Saragovi, H. U. Small peptide mimics of nerve growth factor bind TrkA receptors and affect biological responses. *J. Biol. Chem.* **1995**, *270*, 6564−6569.
(28) Kullander, K.; Ebendal, T. Neurotrophin-3 acquires NGF-like activity after exchange to five NGF amino acid residues: molecular analysis of the sites in NGF mediating the specific interaction with the NGF high affinity receptor. *J. Neurosci. Res.* **1994**, *39*, 195−210.
(29) Ibanez, C. F.; Ilag, L. L.; Murray, R. J.; Persson, H. An extended surface of binding to Trk tyrosine kinase receptors in NGF and BDNF allows the engineering of a multifunctional pan-neurotrophin. *EMBO J.* **1993**, *12*, 2281−2293.
(30) Beglova, N.; LeSauteur, L.; Ekiel, I.; Saragovi, H. U.; Gehring, K. Solution structure and internal motion of a bioactive peptide derived from the nerve growth factor. *J. Biol. Chem.* **1998**, *273*, 23652−23658.
(31) Wiesmann, C.; Ultsch, M. H.; Bass, S. H.; de, V. A. Crystal structure of nerve growth factor in complex with the ligand- binding domain of the TrkA receptor. *Nature* **1999**, *401*, 184−188.
(32) McDonald, N. Q.; Lapatto, R.; Marray-Rust, J.; Gunning, J.; Wlodawer, A.; Blundell, T. L. New protein fold revealed by a 2.3 A resolution crystal structure of nerve growth factor. *Nature* **1991**, *354*, 411−414.
(33) Holland, D. R.; Cousens, L. S.; Meng, W.; Matthews, B. W. Nerve growth factor in different crystal forms displays structural flexibility and reveals zinc binding sites. *J. Mol. Biol.* **1994**, *239*, 385−400.
(34) Hutchinson, E. G.; Thornton, J. M. A revised set of potentials for β-turn formation in proteins. *Protein Sci.* **1994**, *3*, 2207−2216.
(35) Briand, J.-P.; Benkirane, N.; Guichard, G.; Newman, J. F. E.; Van Regenmortel, M. H. V.; Brown, F.; Muller, S. A retro-inverso peptide corresponding to the GH loop of foot-and-moth disease virus elicits high levels of long-lasting protective neutralizing antibodies. *Proc. Natl. Acad. Sci. U.S.A.* **1997**, *94*, 12545−12550.
(36) Wade, D.; Boman, A.; Wahlin, B.; Drain, C. M.; Andreu, D.; Boman, H. G.; Merrifield, R. B. All-D amino acid-containing channel-forming antibiotic peptides. *Proc. Natl. Acad. Sci. U.S.A.* **1990**, *87*, 4761−4765.
(37) Jameson, B. A.; McDonnell, J. M.; Marini, J. C.; Korngold, R. A rationally designed CD4 analogue inhibits experimental allergic encephalomyelitis. *Nature* **1994**, *368*, 744−746.
(38) McDonnell, J. M.; Beavil, A. J.; Mackay, G. A.; Jameson, B. A.; Korngold, R.; Gould, H. J.; Sutton, B. J. Structure based design and characterization of peptides that inhibit IgE binding to its high-affinity receptor. *Nat. Struct. Biol.* **1996**, *3*, 419−426.
(39) McDonnell, J. M.; Fushman, D.; Cahill, S. M.; Sutton, B. J.; Cowburn, D. Solution structure of FceRI α-chain mimics: A β-hairpin peptide and its retroenantiomer. *J. Am. Chem. Soc.* **1997**, *119*, 5321−5328.
(40) Englander, S. W.; Wand, A. J. Main-chain directed strategy for the assignment of the ^{1}H NMR spectra of proteins. *Biochemistry* **1987**, *26*, 5953−5958.
(41) Wüthrich, K. *NMR of Proteins and Nucleic Acids*; Wiley: New York, 1986.
(42) Wilmot, C. M.; Thornton, J. M. β-turns and their distortions: a proposed new nomenclature. *Protein Eng.* **1990**, *3*, 479−493.
(43) Guptasarma, P. Reversal of peptide backbone direction may result in the mirroring of protein structure. *FEBS Lett.* **1992**, *310*, 205−210.
(44) Rose, G. D.; Gierasch, L. M.; Smith, J. A. Turns in peptides and proteins. *Adv. Protein Chem.* **1985**, *37*, 1−109.
(45) LeSauteur, L.; Maliartchouk, S.; Le, J. H.; Quirion, R.; Saragovi, H. U. Potent human p140-TrkA agonists derived from an anti-receptor monoclonal antibody. *J. Neurosci.* **1996**, *16*, 1308−1316.
(46) Maliartchouk, S.; Saragovi, H. U. Optimal nerve growth factor trophic signals mediated by synergy of TrkA and p75 receptor-specific ligands. *J. Neurosci.* **1997**, *17*, 6031−6037.
(47) Mailartchouk, S.; Debeir, T.; Beglova, N.; Cuello, A. C.; Gehring, K.; Saragovi, H. U. Genuine Monovalent Ligands of Nerve Growth Factor Receptors Reveal a Novel Pharmacological Mechanism of Action. *J. Biol. Chem.* **2000**, *275*.
(48) Ibanez, C. F.; Ebendal, T.; Persson, H. Chimeric molecules with multiple neurotrophic activities reveal structural elements determining the specificities of NGF and BDNF. *EMBO J.* **1991**, *10*, 2105−2110.
(49) Ibanez, C. F. Structure−function relationship in the neurotrophin family. *J. Neurobiol.* **1994**, *25*, 1349−1361.
(50) Kullander, K.; Kaplan, D.; Ebendal, T. Two restricted sites on the surface of the nerve growth factor molecule independently determine specific TrkA receptor binding and activation. *J. Biol. Chem.* **1997**, *272*, 9300−9307.
(51) Tian, S.-S.; Lamb, P.; King, A. G.; Miller, S. G.; Kessler, L.; Luengo, J. I.; Averill, L.; Johnson, R. K.; Gleason, J. G.; Pelus, L. M.; Dillon, S. B.; Rosen, J. A small, nonpeptidyl mimic of granulocyte-colony-stimulating factor. *Science* **1998**, *281*, 257−259.
(52) Szewczuk, Z.; Gibbs, B. F.; Yue, S. Y.; Purisima, E. O.; Konishi, Y. Conformationally restricted thrombin inhibitors resistant to proteolytic digestion. *Biochemistry* **1992**, *31*, 9132−9140.
(53) Carver, J. A.; Esposito, G.; Viglino, P.; Fogolari, F.; Guichard, G.; Briand, J. P.; Van Regenmortel, M. H.; Brown, F.; Mascagni, P. Structural comparison between retro-inverso and parent peptides: molecular basis for the biological activity of a retro-inverso analogue of the immunodominant fragment of VP1 coat protein from foot-and-mouth disease virus. *Biopolymers* **1997**, *41*, 569−590.
(54) Ibanez, C. F.; Ebendal, T.; Barbany, G.; Murray, R. J.; Blundell, T. L.; Persson, H. Disruption of the low affinity receptor-binding site in NGF allows neuronal survival and differentiation by binding to the trk gene product. *Cell* **1992**, *69*, 329−341.
(55) Kullander, K.; Kylberg, A.; Ebendal, T. Specificity of neurotrophin-3 determined by loss-of-function mutagenesis. *J. Neurosci. Res.* **1997**, *50*, 496−503.
(56) Urfer, R.; Tsoulfas, P.; O'Connell, L.; Hongo, J. A.; Zhao, W.; Presta, L. G. High-resolution mapping of the binding site of TrkA for nerve growth factor and TrkC for neurotrophin-3 on the second immunoglobulin-like domain of the Trk receptors. *J. Biol. Chem.* **1998**, *273*, 5829−5840.
(57) Saragovi, H. U.; Zheng, W.; Maliartchouk, S.; DiGugliemo, G. M.; Mawal, Y. R.; Kamen, A.; Woo, S. B.; Cuello, A. C.; Debeir, T.; Neet, K. E. A TrkA-selective, fast internalizing nerve growth factor-antibody complex induces trophic but not neuritogenic signals. *J. Biol. Chem.* **1998**, *273*, 34933−34940.
(58) Woo, S. B.; Whalen, C.; Neet, K. E. Characterization of the recombinant extracellular domain of the neurotrophin receptor TrkA and its interaction with nerve growth factor (NGF). *Protein Sci.* **1998**, *7*, 1006−1016.
(59) Nilges, M.; Kuszewski, J.; Brunger, A. T. *Computational aspects of the study of biological macromolecules by NMR*; Plenum Press: New York, 1991.
(60) Nilges, M.; Clore, G. M.; Gronenborn, A. M. Determination of the three-dimensional structures of proteins from interproton distance data by hybrid distance geometry-dynamical simulated annealing calculations. *FEBS Lett.* **1988**, *229*, 317−324.
(61) Kuszewski, J.; Nilges, M.; Brunger, A. T. Sampling and efficiency of metric matrix distance geometry: A novel "partial" metrization algorithm. *J. Biomol. NMR* **1992**, *2*, 33−56.
(62) Brunger, A. T. *X-PLOR version 3.1. A system for crystallography and NMR*; Yale University Press: New Haven, CT, 1992.
(63) Stickle, D. F.; Presta, L. G.; Dill, K. A.; Rose, G. D. Hydrogen bonding in globular proteins. *J. Mol. Biol.* **1992**, *226*, 1143−1159.
(64) Bodenhausen, G.; Ruben, D. J. Natural abundance nitrogen-15 NMR by enhanced heteronuclear spectroscopy. *J. Chem. Phys. Lett.* **1980**, *69*, 185−189.
(65) Palmer, A. G. I.; Rance, M.; Wright, P. E. Intramolecular motion of a zinc finger DNA-binding domain from Xfin characterized by proton-detected natural abundance 13C heteronuclear NMR spectroscopy. *J. Am. Chem. Soc.* **1991**, *113*, 4371−4380.
(66) Lipari, G.; Szabo, A. Model-free approach to the interpretation of nuclear magnetic resonance relaxation in macromolecules. The theory and range of validity. *J. Am. Chem. Soc.* **1982**, *104*, 4546−4559.
(67) Mandel, A. M.; Akke, M.; Palmer, A. G. Backbone dynamics of *Escherichia coli* ribonuclease HI: correlations with structure and function in an active enzyme. *J. Mol. Biol.* **1995**, *246*, 144−163.
(68) Bogenmann, E.; Torres, M.; Matsushima, H. Constitutive N-myc gene expression inhibits trkA mediated neuronal differentiation. *Oncogene* **1995**, *10*, 1915−1925.
(69) Hempstead, B. L.; Rabin, S. J.; Kaplan, L.; Reid, S.; Parada, L. F.; Kaplan, D. R. Overexpression of the trk tyrosine kinase rapidly accelerates nerve growth factor-induced differentiation. *Neuron* **1992**, *9*, 883−896.
(70) Chandler, C. E.; Parsons, L. M.; Hosang, M.; Shooter, E. M. A monoclonal antibody modulates the interaction of NGF with PC12 cells. *J. Biol. Chem.* **1984**, *259*, 6882−6889.

JM990441X